

Received 30 April 2025, accepted 26 May 2025, date of publication 4 June 2025, date of current version 12 June 2025.

Digital Object Identifier 10.1109/ACCESS.2025.3576369



Robust H_{∞} Control Synthesis of a Biomimetic Flapping Wing UAV Operating in Gusty Environment

SADDAM HUSSAIN ABBASI^{®1}, ZAID AHMED SHAMSAN^{®2}, (Senior Member, IEEE), AND NOUMAN ABBASI^{®3}

¹Department of Electrical and Computer Engineering, Sir Syed CASE Institute of Technology (SS-CASE-IT), Islamabad 45230, Pakistan

Corresponding author: Zaid Ahmed Shamsan (zashamsan@imamu.edu.sa)

This work was supported and funded by the Deanship of Scientific Research at Imam Mohammad Ibn Saud Islamic University (IMSIU) (grant number IMSIU-DDRSP2503).

ABSTRACT The Unmanned Aerial Vehicles (UAVs) generally execute their missions in atmospheric boundary layer and this region is highly turbulent which drastically degrades UAVs stability. Drawing inspiration from nature for the solution, it is revealed that natural birds utilize covert feathers to tackle gusts and turbulence. This paper presents design of an active biomimetic Gust Alleviation System (GAS) augmented with robust H_{∞} controller for a flapping wing UAV (FUAV) replicating bird's covert feathers. Reduced order model of the proposed design is computed using bond graph modelling method. Stability analysis is performed to study internal dynamics of the proposed design. A comparison is made between the proposed H_{∞} controller-augmented GAS and Linear quadratic regulator (LQR) controller-based GAS in response to external gust disturbances. The H_{∞} controller augmented GAS design demonstrate more robust behavior of the FUAV compared to LQR based design and successfully alleviates gusts up to 50%. Finally, consistency between the obtained results and literature data confirms the validity of offered H_{∞} controller.

INDEX TERMS Biomimetic, bond graph modeling, gust alleviation system, H_{∞} control, model reduction, robust control, UAV.

I. INTRODUCTION

Unmanned Aerial Vehicles (UAVs) typically carry out their missions in the atmospheric boundary layer, a region characterized by high turbulence that significantly reduces the stability of the UAVs. Hence, in order to carry on functioning of UAVs in windy regions, a Gust Alleviation System (GAS) and biomimetic robust flight controller is requisite to increase the UAV's steady operation in external gusts [1].

Many traditional gust mitigation strategies in UAVs have been examined in detail from available literature. Authors in [2] proposed a design of UAVs with micro-architectureand-control (MARC), which uses state-of-the-art avionics to ensure steady flight of aircraft in the presence of hostile

The associate editor coordinating the review of this manuscript and approving it for publication was Zhiwu Li¹⁰.

winds. Another study depicts that using synthetic jet actuators (SJAs) in UAVs appreciably reduces aerodynamic drag as well as damping of oscillations produced due to gusts, steering towards an enhanced stable aerodynamic behavior [3]. De Rosa et al. [4] proposed a study that explores the utility of vortex generators for load mitigation in UAV wings at the time of high-speed cruising, targeting to defeat wing-tip stall as well as decrease aerodynamic forces in the course of turbulence and gusts. The traditional GAS approaches mentioned above have primarily been investigated for conventional aircraft and fixed-wing micro aerial vehicles (MAVs), while their applicability and effectiveness for flapping-wing UAVs (FUAVs) remain largely unexplored.

In the past ten years, biomimetics has advanced swiftly to tackle engineering challenges. Numerous biologically motivated flow sensors have also been proposed to address

²Electrical Engineering Department, College of Engineering, Imam Mohammad Ibn Saud Islamic University (IMSIU), Riyadh 11432, Saudi Arabia

³National University of Sciences and Technology, Islamabad 44000, Pakistan



turbulence [5], [6]. Another study discovers the idea of feathers motivated compliant airfoils to alleviate turbulence and gust. The authors explore passive camber morphing technique of bird feathers, to lessen aerodynamic gust loads in the presence of turbulent airflow. They proved that these flexible feather-like wings can enhance instant flow control by altering the shape as a retort to changing air flows. The simulation outcomes advocate that feather-inspired strategies can increase stability as well as decrease aerodynamic disturbances produced due to gusts [7]. Nonetheless, the above biologically motivated flow sensors were confined to fixed-wing UAVs only and were not deliberated for flapping wing UAVs. Moreover, augmentation of robust control with biological flow sensors has not been explored so far.

A recent study [8] proposes a biologically inspired "fly-by-feel" control approach that uses wing strain sensors, emulating insect mechanoreceptors, to detect aerodynamic forces and guide flight without conventional inertial sensors. Reinforcement learning is employed to interpret strain data for real-time estimation of attitude and airflow. The system was validated through flight experiments and simulations, including scenarios with wind disturbances varying from 3 m/s to 7 m/s. The results highlight the effectiveness of strain-based feedback in achieving stable and adaptive flight control, offering a promising strategy for gust-resilient operation in flapping-wing UAVs. However, the applicability of the proposed research is limited to wind speeds less than 7 m/s and its utility for higher gust speeds is yet to be done.

In addition to active gust alleviation design techniques several researches have also been carried out till date to alleviate gusts in UAVs using linear and non-linear control strategies. The study in [9] presents a novel airflow sensing method augmented with an adaptive proportional integral derivative (PID) control method to permit efficient and stable flapping drone flight at the time of gusty weather. Trial results establish a 25.15% decrease in root-mean-square errors when exposed to gusts up to 2.4 m/s from front. The offered design increases flight performance and aids as a basis for upcoming progresses in gusty flight of small sized flapping wing drones.

Chirarattananon et al. [10] in their research simulated gusts in a laboratory and examined the outcomes of gusts on flight dynamics of flapping-wing MAV having a millimeterscale size. Simple models depicting the disturbance influence on the MAV dynamics are presented, in addition to two disturbance alleviation strategies able to estimate and compensate for the gust disturbances. The suggested adaptive tracking control designs are validated through experiments. The results enunciate that the proposed design decreased the root-mean-square position errors up to 50% once the MAV is exposed to 80 cm s⁻¹ wind incident in horizontal direction. The flight data further advocates that wing kinematics modulation to achieve stability in flight during gusty weather may subliminally influence an additional stabilization effect, reducing the time-averaged aerodynamic drag faced by the MAV.

Another research in [11] proposed a robust control of a FMAV having a tiered architecture that splits the main controller into three multi-level set of small control arrangements. The lower tier is used to track a desired trajectory, the middle tier ensures stabile flight during incidence of external disturbances, while the top tier enables the MAV to navigate in changing environmental conditions. The proposed controller has effectively achieved smooth flapping flight.

Kim et al. [12] have presented disturbance observer-based controller of FMAV with the main aim of dealing modelling uncertainties. The controller is developed to confirm stable flight during changing aerodynamic settings, including small scale disturbances and parametric uncertainties. A disturbance-observer is combined with a controller to predict external forces including wind gusts and squalls. The presented design counterbalances modelling imprecisions and increases the robustness of the MAV's flight operation. Simulation findings show the efficacy of the design in alleviating the effect of model imperfections and disturbances on the MAV's stability and control.

The authors in [13] offered a Linear Quadratic Regulator (LQR)-based controller strategy for attitude control of a flapping wing drone operating in in gusts. The study though obtained open loop stability, yet it recognized that closed loop controller was required for attitude stability in a gusty airflow, and to preserve flight envelope during turbulence. The LQR control method was able to efficaciously stabilize the drone during gusts measuring up to 3 m/s.

Yu et al. [14] in their recent study address the problem of recovery flight in flapping-wing micro-aerial vehicles (FWMAVs) subjected to extreme attitudes caused by aggressive maneuvers and wind disturbances. The authors propose a reinforcement learning (RL)-based controller that enables the vehicle to regain stable flight while minimizing angular acceleration. To ensure sustained stability after recovery, a hybrid control strategy is introduced by combining the RL controller with a proportional-derivative (PD) controller. Simulation results demonstrate the effectiveness of both the RL and hybrid approaches in managing recovery and stabilization under challenging flight conditions, with future work aimed at real-world implementation.

A recent study in [15] proposes a multi-level optimization model predictive control (MOMPC) framework to address the trade-off between computational cost and control accuracy in flapping-wing micro aerial vehicles (FWMAVs). The authors first construct a quasi-steady aerodynamic model to estimate forces and moments, which are then optimized through a two-layer process: classical MPC for trajectory tracking and an additional optimization layer for refining kinematic parameters. Compared to conventional PID and standard MPC methods, MOMPC demonstrates superior tracking precision and faster response while maintaining stability under gusty wind conditions. The simulation results indicate that MOMPC maintains good control accuracy; however, the emergence of gusty winds increases the tracking



errors between reference signals and actual system states. These findings confirm MOMPC's effectiveness and robustness for real-time control of FWMAVs in nonlinear and constrained environments. However, the FWMAVs stability during higher gusts need further research.

All the control strategies studied so far are efficient in alleviating small disturbances and winds only and lack the ability to effectively tackle larger gusts. The main reason is that most of the proposed control strategies are used to alleviate gust in isolation without use of any active gust alleviation design to augment the control synthesis. The same is observed by Fang. et al. [16] and they have proposed that the prevalent single-control designs can barely fulfil the flight control demands of a flapping drone in varying flight modes and multiple tasks underneath a highly nonlinear and highly dynamic system. Therefore, they suggest that the latest controllers of the flapping drones need to be augmented with some active design techniques such as feathers designs or developing a complex multi-control strategy comprising multiple control modules performing tasks in parallel for improved gust alleviation performance. In addition, emerging sliding mode control strategies, including adaptive integral and predictor-based fixed-time approaches, offer improved robustness in handling external disturbances, particularly in maneuvering scenarios [27].

Taking lead from this finding, nature has been referred for probable solution to handle gusts effectively. In-depth research on natural flyers has revealed that transition to an intermittent flight is resorted by them when exposed to gusty airflows and turbulent weather conditions. During this non-flapping time period, they usually either loiter or start gliding. The covert feathers come in to action immediately and open up in these non-flapping gusty flying states to reduce adverse effects of turbulence and gusts, as illustrated in Fig. 1 [6].

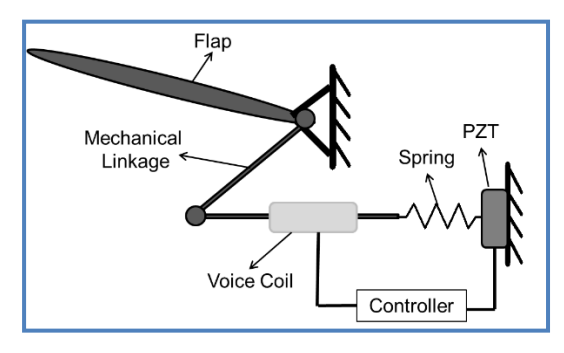


FIGURE 1. Covert feathers in birds [6].

Drawing from the avian's covert hidden feathers, authors in their early studies [17], [18], [19] introduced an innovative biomimetic gust alleviation system (GAS) for flapping wing UAV (FUAV). The GAS is made up of electromechanical (EM) covert feathers which are merged into both wings of the UAV. The GAS is activated solely during turbulent weather to dissipate gusts, and in normal weather scenarios, it remained

fixed to the UAV wing to uphold the airfoil's fundamental shape. It offered numerous advantages in flight, to include enhanced stability in challenging weather conditions.

In this study, we build upon the previous research by presenting GAS comprising 16 feathers. We then integrate this GAS into the flapping wing of FUAV, which we approximate as a rigid beam and develop wing model suitable for gust alleviation. Further to lessen the computational complications, we perform the model order reduction (MOR) to obtain a simplified seventh-order model. A stability analysis is carried out, which necessitates the augmentation of an active control system based on H_{∞} robust controller to ensure the smooth and robust operation of the FUAV during gust disturbances. Comparison of the developed H_{∞} robust controller is made with LQR controller and robustness of both control techniques is studied. Finally, the consistency between the results obtained from the proposed active GAS augmented with the robust H_{∞} controller and literature data is examined to ensure the correctness of the offered H_{∞} controller design. While existing literature typically addresses either active gust alleviation systems or control techniques independently, this work uniquely combines a biologically inspired covert feather-based GAS with H_{∞} robust control, a novel integration not previously reported and a key contribution of this study.

The paper is further structured as follows: Part 2 discusses the FUAV GAS architecture and the formulation of reduced order bond graph model of a GAS. Part 3 covers stability studies, and the H_{∞} robust controller design is presented in part 4. Part 5 presents the simulation findings, and the final part contains the conclusions.

II. DYNAMIC MODEL

The baseline UAV selected for current study is the FESTO Flapping Bird [20]. The proposed GAS comprises 16 covert EM feathers. Half of these EM feathers are positioned on the upper surface of the wing, and the rest are on the lower surface. Each EM feather includes a bio-inspired controller, flap, voice coil actuator, encoder, piezoelectric transducer (PZT), mechanical link, and spring. The structure of the EM covert feather is illustrated in Fig. 2. For additional design specifications of EM feathers, the author's earlier study [18] can be consulted.



FIGURE 2. Electromechanical covert feather [18].



Bond graph representation is a visual depiction of dynamic systems, concentrating on power transfer among subsystem elements. It employs a collection of components to include junctions, bonds, and energy storage elements to simulate evolving systems. This method facilitates the structured evaluation of multi-domain models (electrical, mechanical, hydraulic etc.), proving beneficial in automation and controls [21]. The intended GAS architecture is a multi-domain structure; therefore, bond graph modeling is used in this research to develop a mathematical model. First of all, the bond graph model of a single feather is developed, then bond graph model of rigid wing is constructed, later both of these models are combined and enhanced to make a final 16 feathers wing bond graph model dovetailed with GAS which is shown in Fig. 3. The values of all the elements of bond graph model of the GAS are chosen from the author's earlier research [17]. Stepwise thorough development of these bond graph models is not included here and the interested readers are encouraged reading of author's following works [17], [18].

A. BOND GRAPH MODEL OF RIGID WING

Wings' modeling is carried out by considering them as a rigid beam undergoing a transverse motion. It is assumed to be pivoted at one end. Therefore, the end point displacement in vertical direction is given by [17]:

$$y = l \sin \theta \tag{1}$$

where θ is flapping angle, y is the displacement and l is the span of wing. The flow and effort relationship is as given below [18]:

$$V_{v} = (lcos\theta)\omega \tag{2}$$

$$F = \tau / (x_1 \cos \theta) \tag{3}$$

where F represents force, V_y shows the upward velocity and torque is given by τ . Finally, the bond graph model (BGM) of wing under gust (Sf) is shown in Figure 3. $x_1\cos x_1\cos \theta$ and $l\cos\theta$ are the transformer modulus (TF).

B. BOND GRAPH MODEL OF SINGLE FEATHER

The mathematical equations of a single feather attained through bond graph model shown in figure 3 are given in equations (4) to (11). The state variables are p_1 , p_2 , p_3 that are the generalized momentum of inertia elements and q_1 , q_2 , q_3 , q_4 that are the generalized displacement of compliance elements.

$$\dot{p_1} = ic \cdot p_3 + ic \cdot q_3 \tag{4}$$

$$\dot{q_1} = \frac{1}{I_1} \cdot p_2 \tag{5}$$

$$\dot{p_2} = \frac{ic}{l}p_3 + \frac{ic}{l}q_3 - \frac{1}{C}q_1 - \frac{1}{C_1}q_2 - \frac{m}{C_2}q_4$$
 (6)

$$\dot{q_2} = \frac{1}{I_1} \cdot p_2 \tag{7}$$

$$\dot{p}_3 = q_5 \tag{8}$$

$$\dot{q_3} = S_f - \frac{1}{l \cdot I_1} p_2 - \frac{1}{l} p_1 \tag{9}$$

$$\dot{q_4} = \frac{m}{I_1} p_2 - \frac{R}{C_2} q_4 \tag{10}$$

$$\dot{q_5} = \frac{1}{l \cdot l_1} p_2 \tag{11}$$

C. BOND GRAPH MODEL OF GAS INSTALLED RIGID WING

Modeling of a single feather helps us obtain the BGM of a GAS comprising 16 EM feathers. Finally, the GAS model and rigid wing model helps us form the BGM of a complete GAS incorporated flapping wing and is shown in figure 3. It is acquired by adding GAS BGM to the rigid wing BGM by the use of a transformer. The mathematical representation of the entire wing and GAS results in 134^{th} -order state space model. The state vector $\vec{x}(t)$ consists of generalized momentum at all inertia elements and generalized displacement at all compliance elements.

Balanced Truncation reduced order modeling approach is applied to compute a lower rank approximation of the 134th-order mathematical model as the same is computationally complex for control synthesis purposes. Balanced truncation method works by transforming the system into a special coordinate space where each state is ranked based on its combined controllability and observability quantified using Hankel Singular Values (HSVs). States with large HSVs contribute significantly to the system's input-output behavior, while those with small HSVs have minimal impact. The low-impact states are then discarded, resulting in a reduced-order model (ROM) that maintains high fidelity to the original system [19]. Figure 4 shows the HSVs based states energy of the seventh order reduced model computed using balanced truncation method in MATLAB. The bode plots of the full-order model (FOM) and ROM is shown in Fig. 5. The plots exhibit close agreement across low to mid frequencies, with minor deviations appearing only at higher frequencies. These high-frequency discrepancies are negligible, as they correspond to system states with low HSVs and minimal energy contribution. This validates that the ROM retains dominant system dynamics and ensures fidelity. The final ROM has seven states namely the generalized displacement of flaps of feathers f_1 , f_3 , f_4 , f_6 , f_7 , f_8 , and f_9 and the state vector is $\mathbf{x} = [\mathbf{q}_{f1} \ \mathbf{q}_{f3} \ \mathbf{q}_{f4} \ \mathbf{q}_{f6} \ \mathbf{q}_{f7} \ \mathbf{q}_{f8} \ \mathbf{q}_{f9}]^T$. The generalized depiction of the state space formulation thus obtained is: -

$$\vec{x}(t) = A \cdot \vec{x}(t) + B \cdot \vec{u}(t) + B_d \cdot \vec{w}(t)$$

$$\vec{y}(t) = C \cdot \vec{x}(t) + D \cdot \vec{u}(t)$$
(12)

where $\vec{w}(t)$ represents wind gust and B_d denotes gust influence. The final reduced order of the system's state matrix A is 7×7 , the reduced order of the input gain matrix B is 7×1 and the reduced order of output gain matrix C is 1×7 .

III. STABILITY ASSESSMENT

Stability assessment of the reduced system model is performed in this section. Table 1 depicts the poles of the system



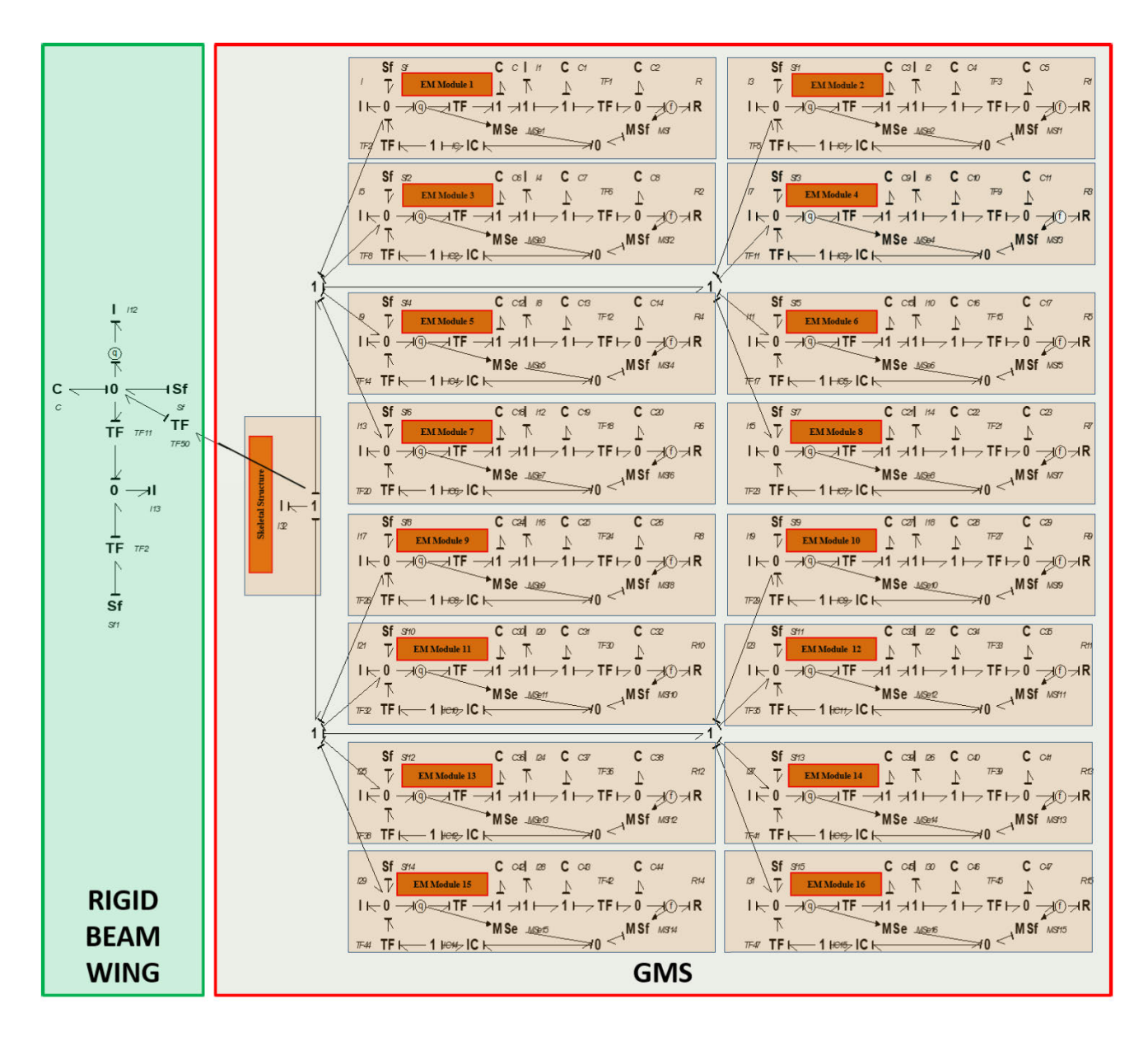


FIGURE 3. Bond graph model of a wing with GAS [19].

and enunciates that the system is unstable as one pole is in the right half plane. In addition, the step response also blows up. The unstable state response of the open loop system subjected to gusts is shown in Fig. 6. This unstable behavior necessitates development of a robust controller to ensure attitude stability during gusts. The system is fully controllable with controllability of 7.

$$A = \begin{bmatrix} -8.8 & -2.5 & -3.3 & 1.8 & 5.1 & -3.1 & -6.1 \\ -9.9 & -1.2 & -9.1 & 2.05 & 2.6 & -4.2 & -6.7 \\ -5.03 & 7.5 & -4.7 & 3.5 & -4.1 & 0 & -7.6 \\ -9.3 & 3.3 & -2.9 & -1.5 & -6.5 & 6.1 & 4.9 \\ 3.1 & 4.1 & -3 & -1.9 & -8.1 & 3.4 & 6.4 \\ 0 & -6.4 & 0 & 7.2 & 3.3 & -0.04 & -2.9 \\ -4.4 & 0.4 & -1.4 & 1.2 & -0.7 & -3.5 & -4.03 \end{bmatrix}$$

B =
$$\begin{bmatrix} 2.9 & 3.2 & 0 & -3.4 & 0.21 & 0 & -0.9 \end{bmatrix}^T$$

C = $\begin{bmatrix} 0.07 & 4.32 & 0 & -0.06 & 0.1 & 0 & 1.9 \end{bmatrix}$ D = $\begin{bmatrix} 0 \end{bmatrix}$

IV. ROBUST H_{∞} CONTROL SYNTHESIS

In this part we shall develop GAS controller basing on robust control that is introduced as a H_{∞} control. The closed loop H_{∞} control block diagram is illustrated in Fig. 7. The H_{∞} control is a robust control technique employed to create controllers that enhance system performance while reducing the influence of external disturbances and model uncertainties. It is especially beneficial in systems where uncertainty or external disturbances are substantial and need to be considered in the overall controller design [22]. Since the proposed GAS design is primarily for operation in external disturbance,



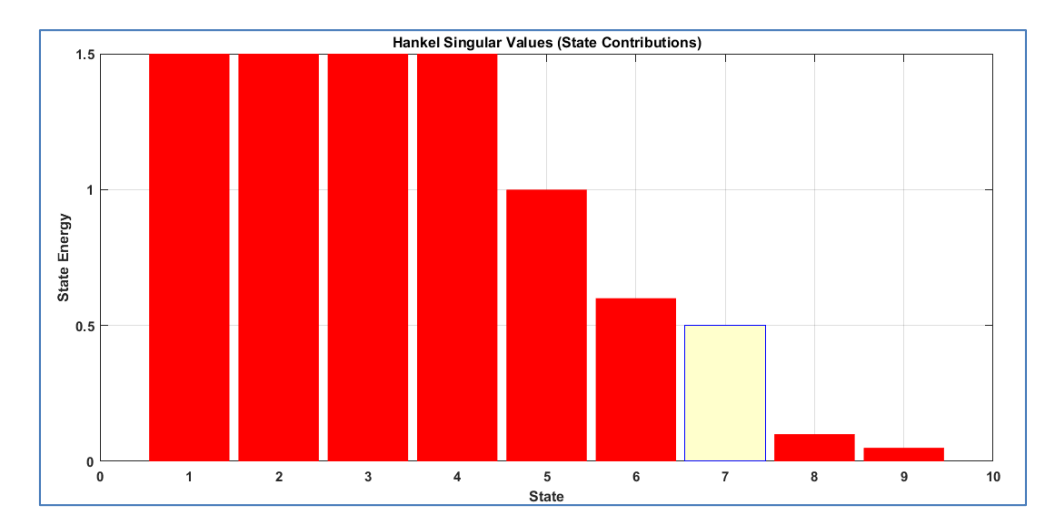


FIGURE 4. State energy of the ROM.

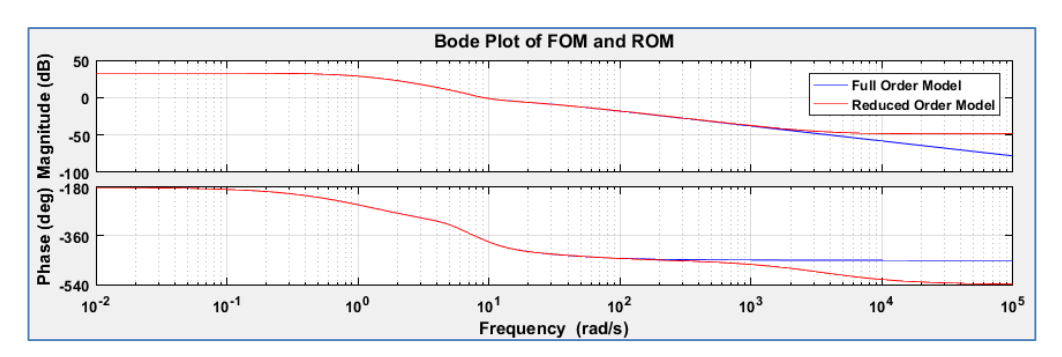


FIGURE 5. Bode plot of FOM and ROM.

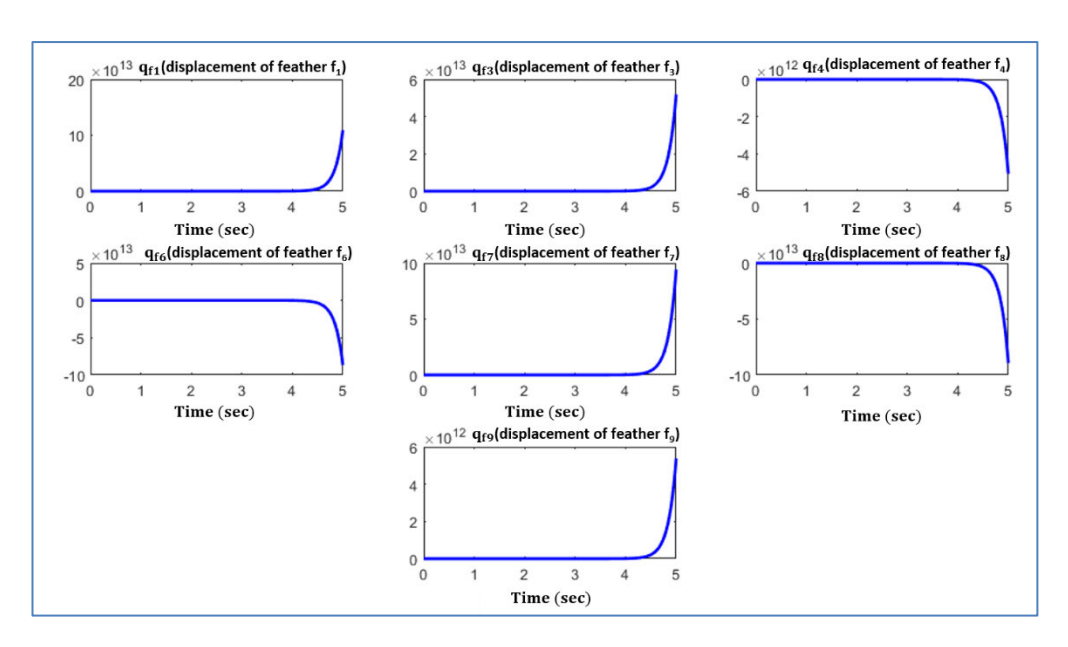


FIGURE 6. Open loop states response to gust.

that is, gust therefore the H_{∞} control approach is presented in this study. Moreover, the results will be compared to the LQR controller for GAS.

In the preceding diagram, G represents the plant, K stands for the controller, y denotes the measurement, w signifies the disturbance, u indicates the controller signal, and z is



| TABLE | 1 Open | loop eige | nvaluos |
|-------|--------|------------|----------|
| IABLE | . Oben | ioob eigei | nvaiues. |

| | Poles | ζ | ω _n | Eigenvectors | |
|-------------|-----------|-----|----------------|---|--|
| | | | | <u> </u> | |
| λ_I | -20 | 1 | 20 | [2.86 2.53 -0.35 -0.88 -2.82 1.72 1] | |
| λ_2 | 6.4 | -1 | 6.4 | [0.15 1.23 -0.62 -1.8 0.37 -3.4 1] | |
| λ3,4 | -2.6±5.3j | 0.4 | 5.4 | [0.7±0.25j 2.46±3.12j -2.11±2.42j 2.13±1.24j 1.56±2.54j 0.26±0.48j] | |
| λ_5 | -5.8 | 1 | 5.8 | [-1.12 1.68 1.84 -0.07 3.03 0.73 1] | |
| λ_6 | -0.91 | 1 | 0.9 | [-0.14 1 0.07 0.94 0.89 -0.48 1] | |
| λ_7 | -2.6 | 1 | 2.6 | [-0.12 1.35 0.32 1 1.46 -0.18 1] | |

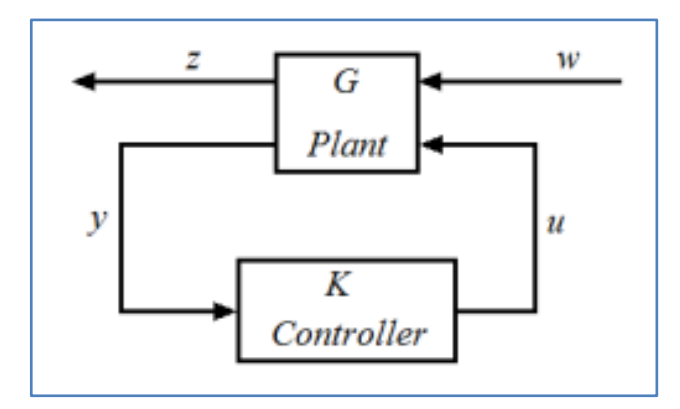


FIGURE 7. H_{∞} robust control block diagram.

the controller signals array containing all regulated signals. H_{∞} controller reduces the H_{∞} norm [23]. To design the H_{∞} controller, initially a transfer function is formulated which is given as follows: -

$$G(s) = \begin{bmatrix} A & B_w & B_u \\ C_y & 0 & D_{yu} \\ C_m & D_{mw} & o \end{bmatrix}$$
 (13)

There are certain assumptions that are required to be met before further development of the H_{∞} controller [24]. These assumptions are appended as follows: -

- (A,B_u) is stabilizable and (C_m,A) is detectable.
- $D_{yu}^* \times [C_y D_{yu}] = [0 I]$

$$\bullet \ \left[\begin{array}{c} B_w \\ D_{mw} \end{array} \right] \times D_{mw}^* = \left[\begin{array}{c} 0 \\ I \end{array} \right]$$

- $\begin{bmatrix} A j\omega I & B_u \\ C_y & D_{yu} \end{bmatrix}$ has full column rank for all ω
- $\begin{bmatrix} A-j\omega I & B_w \\ C_m & D_{mw} \end{bmatrix}$ has full column rank for all ω

Meeting the above assumptions will guarantee the development of H_{∞} controller properly. The general solution of H_{∞} controller comprises two Hamiltonian matrices that are given

in equation (14) and (15) [25].

$$H_{\infty} = \begin{bmatrix} A & \gamma^{-2} B_w B_w^* - B_u B_u^* \\ -C_y^* C_y & -A^* \end{bmatrix}$$

$$J_{\infty} = \begin{bmatrix} A^* & \gamma^{-2} C_y^* C_y - C_m^* C_m \\ -B_w B_w^* & -A \end{bmatrix}$$
(14)

$$J_{\infty} = \begin{bmatrix} A^* & \gamma^{-2} C_y^* C_y - C_m^* C_m \\ -B_w B_w^* & -A \end{bmatrix}$$
 (15)

Once the above two Hamiltonian matrices are successfully calculated, then we need to compute the values of X_{∞} and Y_{∞} utilizing the equations (16) and (17) [26].

$$X_{\infty} = Ric(H_{\infty}) \tag{16}$$

$$Y_{\infty} = Ric(J_{\infty}) \tag{17}$$

Finally, the H_{∞} robust controller gain is calculated as: -

$$K_{\infty} = -B_{u}^{*}X_{\infty} \tag{18}$$

V. SIMULATIN STUDIES

The developed model of the gust alleviation system along with the allied robust H_{∞} controller is simulated and the results are presented in this part. Covert feather number 2 of the GAS is examined as a case study to provide a clearer understanding of the GAS system's internal dynamical behavior. From the bond graph model in Fig. 3, the modulated effort source (MSe1), which represents the force acting on mechanical linkage for feather 1, serves as the input component, whereas the output component is the resulting force acting on flap (I3) of feather 1. Linearizing the model against this input output components in the 20-Sim simulation software generates a single input single output state space model appended in part 2 of the paper. The reduced seventh order model of the UAV wing with GAS is further simulated in MATLAB software by incidence of different vertical step gust inputs of values 16 m/s, 19 m/s, 22 m/s and 25 m/s. The step response of the designed controller is compared to the LQR controller subjected to above mentioned gust intensities and are shown in Fig. 8. The characteristics of the step response plots of LQR controller compared to the proposed robust H_{∞} controller is summarized in table 2.



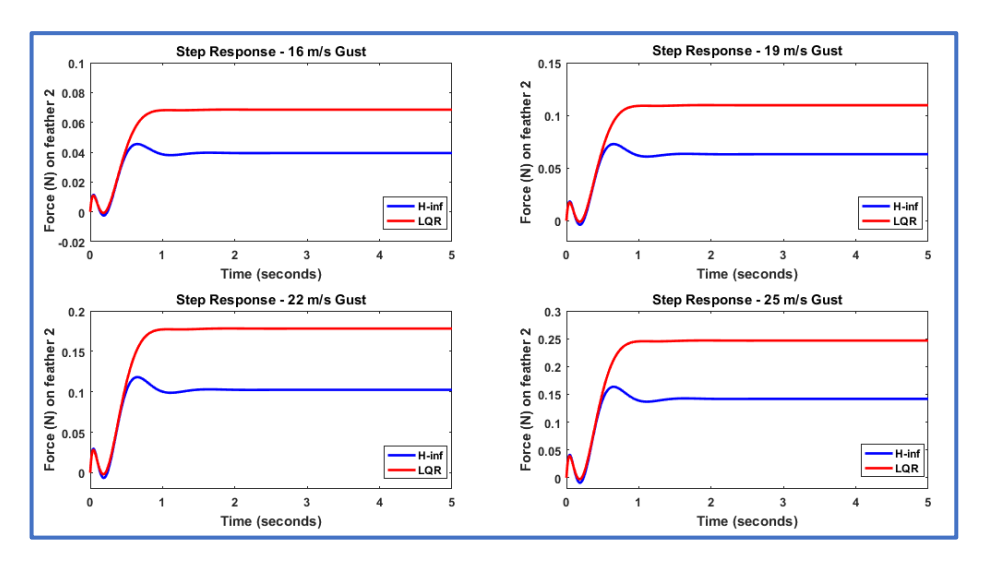


FIGURE 8. Step response comparison of the proposed H_{∞} robust control vs LQR at different gust intensities.

TABLE 2. Step response characteristics of the proposed robust H_{∞} controller vs LQR controller.

| Gust Speed (m/s) | Rise Time (sec) | | Settling Time (sec) | | Peak Value (N) | | Steady State (N) | |
|---------------------|-----------------|------|---------------------|------|----------------|------|------------------|------|
| | H_{∞} | LQR | H_{∞} | LQR | H_{∞} | LQR | H_{∞} | LQR |
| 16 | 0.46 | 0.68 | 1.17 | 0.96 | 0.05 | 0.07 | 0.04 | 0.07 |
| 19 | 0.46 | 0.68 | 1.17 | 0.96 | 0.07 | 0.11 | 0.06 | 0.11 |
| 22 | 0.46 | 0.68 | 1.17 | 0.96 | 0.12 | 0.18 | 0.10 | 0.18 |
| 25 | 0.46 | 0.68 | 1.17 | 0.96 | 0.16 | 0.25 | 0.14 | 0.25 |

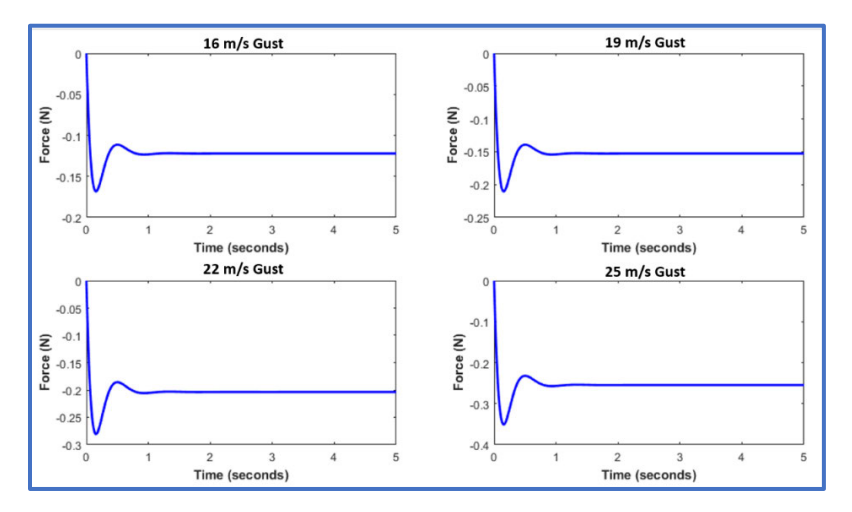


FIGURE 9. Control input response of the proposed H_{∞} robust control at different gust speeds.

Figure 8 clearly enunciates that both controllers have successfully stabilized the unstable GAS model. Moreover, the Robust H_{∞} controller consistently shows a lower rise

time of 0.46 seconds compared to the LQR controller rise time of 0.68 seconds. This suggests that the H_{∞} controller reacts more quickly to external disturbance across all gust

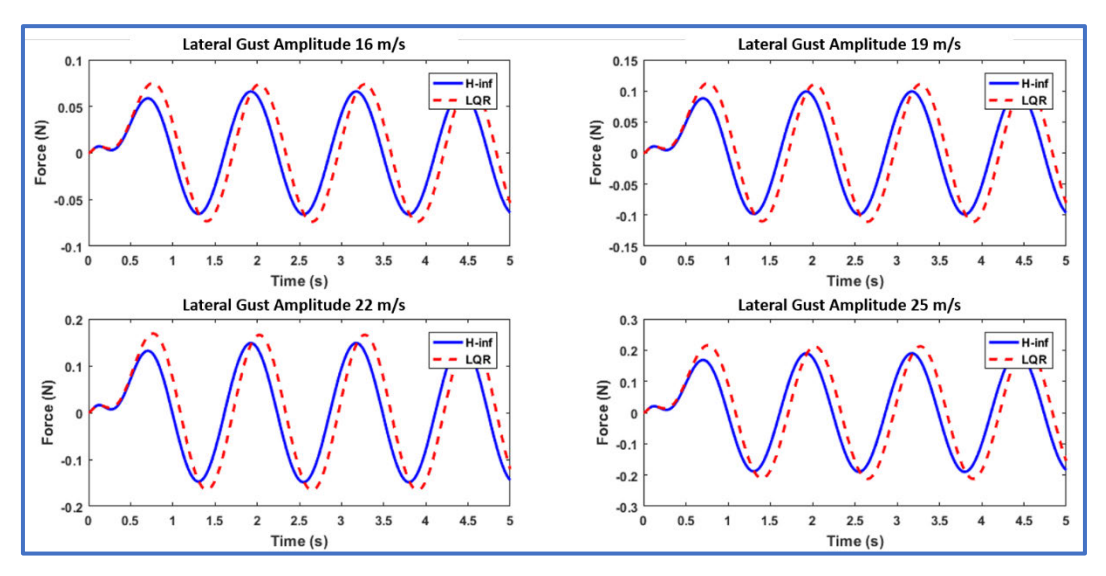


FIGURE 10. Response comparison of the proposed H_{∞} robust controller vs LQR at different lateral sinusoidal gust intensities.

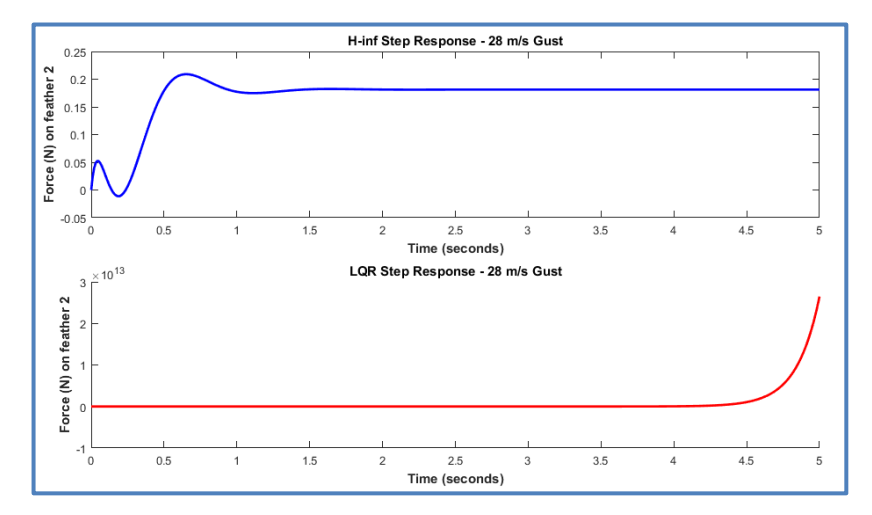


FIGURE 11. Step response comparison of the proposed H_{∞} robust control vs LQR at 28 m/s gust.

speeds in comparison to LQR controller therefore advocating robustness of proposed H_{∞} controller. The peak values of the system's response under the robust H_{∞} controller are consistently lower than those under the LQR controller across all gust speeds. For example, at a gust speed of 25 m/s, the peak value for the H_{∞} controller is 0.16 N, while for LQR controller, it is 0.25 N. This proves that the H_{∞} controller results in less overshoot which is an indicator of a more stable and controlled response. The steady state values of the system's response under the robust H_{∞} controller are steadily lower than those under the LQR controller across all gust speeds. For example, at a gust speed of 25 m/s, the steady state value for H_{∞} controller is 0.14 N, while for LQR controller, it is 0.25 N. This proves that the proposed H_{∞} controller for the under study FUAV shows more robust performance when subjected to external gust disturbances. The settling

time of the LQR controller is 0.96 seconds whereas for the robust H_{∞} controller is 1.17 seconds which depicts advantage of LQR over the H_{∞} controller. To summarize, the H_{∞} controller shows overall more robust performance against external gust disturbances compared to the LQR. Moreover, the stabilization time of the proposed robust H_{∞} controller matches with the settling time of the FUAV under gust found in literature [15]. The control input response of the proposed H_{∞} robust control at different gust speeds is illustrated in Fig. 9.

The FUAV GAS model is now subjected to lateral sinusoidal gusts with amplitudes of 16 m/s, 19 m/s, 22 m/s and 25 m/s and response comparison of the proposed robust H_{∞} controller-based GAS and LQR controller-based GAS is shown in Fig. 10. The response enunciates that the H_{∞} controller reacts more quickly to lateral sinusoidal



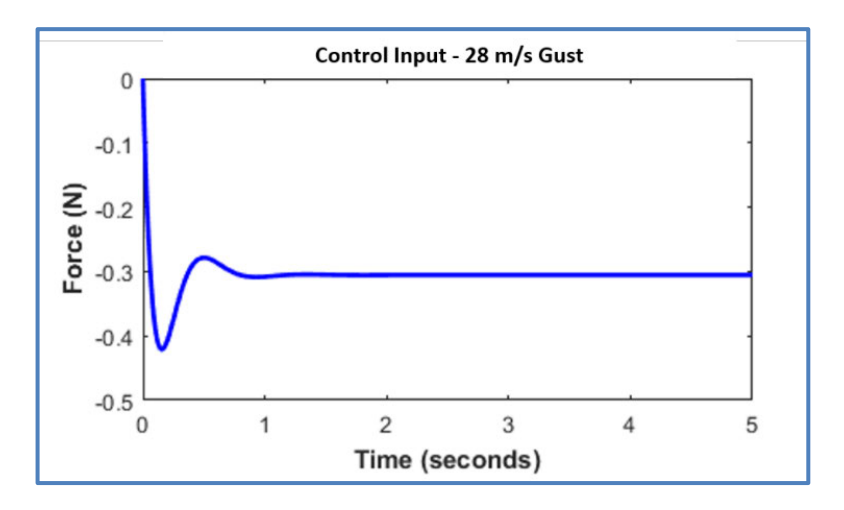


FIGURE 12. Control input response of the proposed H_{∞} robust control at 28 m/s gust.

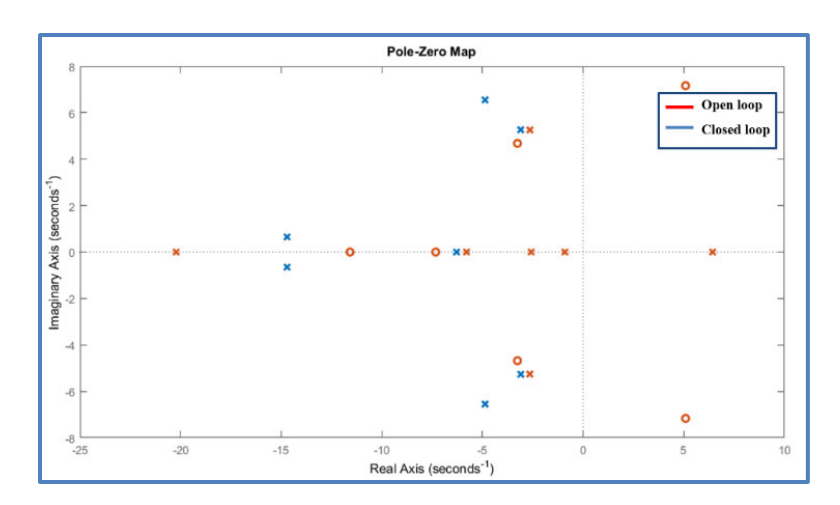


FIGURE 13. Pole-zero map of the closed loop system.

disturbance across all gust speeds in comparison to LQR controller therefore advocating robustness of the proposed H_{∞} controller-augmented GAS. For example, under a lateral sinusoidal gust of 25 m/s amplitude, the H_{∞} controller exhibits superior suppression characteristics. Quantitatively, the peak output of H_{∞} is 0.190 N whereas LQR has 0.216 N peak output. Similarly, root mean square output of H_{∞} is 0.126 N and that of LQR is 0.143 N. This confirms that the proposed H_{∞} controller offers improved robustness and disturbance attenuation for persistent lateral gusts.

Now the GAS model is subjected to 28 m/s vertical step gust and the response of both the controllers is shown in Fig. 11. It can be seen that the step response is converging for the proposed robust H_{∞} controller meaning that the controller has successfully stabilized the unstable GAS even at 28 m/s gust, whereas the step response of LQR controller under input constraints is diverging depicting that the LQR controller has failed to stabilize the FUAV. The controller gain computed is $K_{\infty} = [0.36\ 2.95\ -1.50\ -4.33\ 0.89\ -8.37\ 2.40]$. The control

input plot of the robust H_{∞} controller at 28 m/s gust is shown in Fig. 12.

The robust H_{∞} controller closed loop eigenvalues and the related natural frequency and damping ratio of each eigen value are appended in Table 3. It is evident that the robust H_{∞} controller design of the GAS has successfully made the unstable open-loop eigenvalue stable by relocating it from the right half plan to left half plan, while the eigenvalues already in the left half plan have been augmented, thus significantly decreasing the settling time. The open loop

TABLE 3. Closed loop eigenvalues.

| Poles | ζ | $\omega_{\rm n}$ |
|------------|-----|------------------|
| - 6.2 | 1 | 6.2 |
| -4.8±6.5j | 0.6 | 8.1 |
| -14.7±0.6j | 1 | 14.7 |
| -3.1±5.2j | 0.5 | 6.1 |

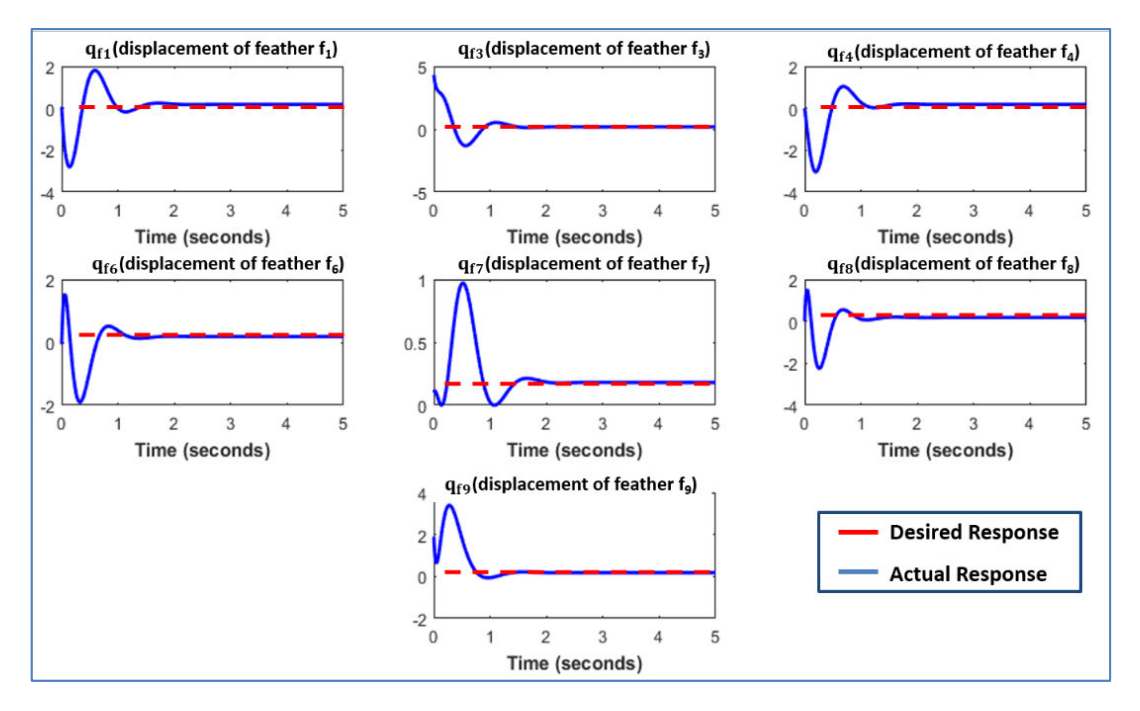


FIGURE 14. Closed loop states response to 28 m/s gust.

and the closed loop pole-zero map is illustrated in Fig. 13. Further, Lyapunov's direct method is used to validate the asymptotic stability of the closed-loop system under the H_{∞} controller. The continuous-time Lyapunov equation given in equation (19) is solved using MATLAB, with Q=I as a positive definite matrix. The solution matrix P is found to be positive definite, with eigenvalues of $P=[0.0213\ 0.0388\ 0.0730\ 0.0884\ 0.2610\ 1.1052\ 1.2268]$. This confirms that a valid Lyapunov function exists and therefore proves that the closed-loop system is asymptotically stable.

$$A_{cl}^T P + P A_{cl} = -Q (19)$$

The dynamic states response of the closed loop GAS with the H_{∞} Robust Control when subjected to 28 m/s gust is depicted in Fig. 14, which illustrates that all the internal states have stabilized in less than 1.5 seconds. This stabilization time matches the states stabilization times in the experimental study by [15] and also by [27]. The same validates the correctness of the designed robust controller.

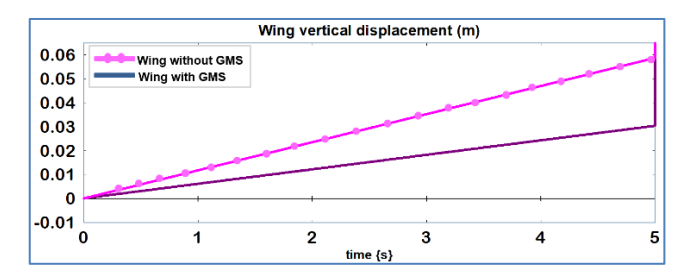


FIGURE 15. Wing vertical displacement at 25 m/s gust.

Moreover, the displacement in vertical direction of the flapping wing having no GAS and the wing having GAS augmented with H_{∞} robust control tested at 25 m/s gust is demonstrated in Fig. 15. The simulation enunciates successful alleviation of gust up to 50% due to feathers actuation in the GAS. This successfully certifies the efficiency of the proposed GAS augmented with the H_{∞} robust control in tackling gusts.

VI. CONCLUSION

We present the design of an active biomimetic Gust Alleviation System (GAS) augmented with a robust H_{∞} controller for a flapping wing UAV (FUAV) replicating bird's covert feathers. A reduced seventh order model of the proposed design is computed using the bond graph modelling method. Stability analysis is carried out, which reveals unstable internal dynamics of the proposed design which necessitates development of a controller. To address the external gust disturbances, affecting the stable flight of the FUAV, an H_{∞} based robust controller is synthesized. A comparison of the proposed H_{∞} controller augmented GAS is made with the LQR controller-based GAS against the external gust disturbances. The H_{∞} controller augmented GAS design shows more robust behavior of the FUAV compared to the LQR based design and successfully alleviates gusts by up to 50% at 25 m/s. In addition, the designed controller successfully brings all poles in the left half plan, and the step response also converges, which proves stable closed loop behaviour. The states plot at a gust speed of 28 m/s shows that all states converge to stability in 1.5 seconds. Furthermore, the simulation results align with previously published literature, certifying



the efficacy of the proposed robust H_{∞} controller augmented GAS design for FUAV, compared to the LQR-based GAS design.

The future research extending the current findings is planned, which includes computational fluid dynamic modeling of the presented GAS design for a detailed aerodynamics investigation. Designing of techniques to handle modeling uncertainties and parametric variations will be studied. A high-gain observer (HGO) design will be developed to estimate the internal dynamic states of the GAS, using input and output measurements. Moreover, data-driven control techniques, including deep learning and reinforcement learning methodologies, will be explored to handle external disturbances, particularly gusts. Finally, the physical construction of the FUAV equipped with the GAS will be undertaken, with careful consideration of practical challenges such as actuation mechanisms, sensing reliability under high gusts, and power limitations.

REFERENCES

- S. Izzal Azid, S. Ahmad Ali, M. Kumar, M. Cirrincione, and A. Fagiolini, "Precise trajectory tracking of multi-rotor UAVs using wind disturbance rejection approach," *IEEE Access*, vol. 11, pp. 91796–91806, 2023, doi: 10.1109/ACCESS.2023.3308297.
- [2] J. Ratti, J.-H. Moon, and G. Vachtsevanos, "Towards low-power, low-profile avionics architecture and control for micro aerial vehicles," in *Proc. Aerosp. Conf.*, Mar. 2011, pp. 1–8, doi: 10.1109/AERO.2011.5747444.
- [3] A. R. Salih, M. O. O. Ibrahim, and J. S. B. M. Aziz, "Effect of synthetic jet actuators on UAV aerodynamic performance," *IEEE Access*, vol. 8, pp. 156245–156257, 2020, doi: 10.1109/ACCESS.2020.3011139.
- [4] D. de Rosa, C. De Michele, and P. Catalano, "Impact of micro vortex generators on aerodynamic performance," in *Proc. AIAA SCITECH Forum*, Jan. 2025, pp. 1–16.
- [5] K. C. Tejaswi, C.-K. Kang, and T. Lee, "Dynamics and control of a flapping wing UAV with abdomen undulation inspired by monarch butterfly," in *Proc. Amer. Control Conf. (ACC)*, May 2021, pp. 66–71, doi: 10.23919/ACC50511.2021.9483293.
- [6] D. Bechert, M. Bruse, W. Hage, R. Meyer, D. Bechert, M. Bruse, W. Hage, and R. Meyer, "Biological surfaces and their technological application–laboratory and flight experiments on drag reduction and separation control," in *Proc. 28th Fluid Dyn. Conf.*, Jun. 1997, pp. 1–18, doi: 10.2514/6.1997-1960.
- [7] L. L. Gamble, C. Harvey, and D. J. Inman, "Load alleviation of feather-inspired compliant airfoils for instantaneous flow control," *Bioinspiration Biomimetics*, vol. 15, no. 5, Oct. 2020, Art. no. 056010, doi: 10.1088/1748-3190/ab9b6f.
- [8] T. Kim et al., "Wing-strain-based flight control of flapping-wing drones through reinforcement learning," *Nature Mach. Intell.*, vol. 6, no. 9, pp. 992–1005, Sep. 2024, doi: 10.1038/s42256-024-00893-9.
- [9] C. Wang, S. Wang, G. De Croon, and S. Hamaza, "Embodied airflow sensing for improved in-gust flight of flapping wing MAVs," *Frontiers Robot. AI*, vol. 9, Dec. 2022, Art. no. 1060933, doi: 10.3389/frobt.2022.1060933.
- [10] P. Chirarattananon, Y. Chen, E. F. Helbling, K. Y. Ma, R. Cheng, and R. J. Wood, "Dynamics and flight control of a flapping-wing robotic insect in the presence of wind gusts," *Interface Focus*, vol. 7, no. 1, Feb. 2017, Art. no. 20160080, doi: 10.1098/rsfs.2016.0080.
- [11] B. Tarvirdizadeh, A. Yousefi-Koma, and E. Khanmirza, "Robust control of flapping-wing in micro aerial vehicle to have a smooth flapping motion," *GSTF J. Aviation Technol.*, vol. 1, no. 1, pp. 1–16, Mar. 2014, doi: 10.5176/2382-5758_1.1.3.
- [12] I. Kim, H. Park, S. Kim, J. Suk, and S. Cho, "Disturbance observer-based control design of flapping-wing MAV considering model uncertainties," Melbourne, VIC, Australia, Nov. 2018, pp. 1–9.
- [13] M. Bhatia, M. Patil, and C. Woolsey, "Stabilization of flapping-wing micro-air vehicles in gust environments," *J. Guid. Control Dyn.*, vol. 37, no. 2, pp. 1–8, Mar.-Apr. 2014.

- [14] Y. Yu, Q. Lu, and B. Zhang, "Reinforcement learning based recovery flight control for flapping-wing micro-aerial vehicles under extreme attitudes," *Int. J. Adv. Robotic Syst.*, vol. 22, no. 1, Jan. 2025, Art. no. 17298806241303290, doi: 10.1177/17298806241303290.
- [15] H. Zheng, W. Chen, and F. Xie, "Control simulation of flapping-wing micro aerial vehicle based on multi-level optimization model predictive control," *IEEE Access*, vol. 12, pp. 40700–40709, 2024, doi: 10.1109/ACCESS.2024.3376646.
- [16] X. Fang, Y. Wen, Z. Gao, K. Gao, Q. Luo, H. Peng, and R. Du, "Review of the flight control method of a bird-like flapping-wing air vehicle," *Micro-machines*, vol. 14, no. 8, p. 1547, Jul. 2023, doi: 10.3390/mi14081547.
- [17] S. H. Abbasi and A. Mahmood, "Bio-inspired gust mitigation system for a flapping wing UAV: Modeling and simulation," *J. Brazilian Soc. Mech. Sci. Eng.*, vol. 41, no. 11, p. 524, Nov. 2019, doi: 10.1007/s40430-019-2044-9
- [18] S. H. Abbasi, A. Mahmood, A. Khaliq, and M. Imran, "Reduced order modeling and simulation of a bio-inspired gust mitigating flapping wing UAV," *Int. J. Intell. Robot. Appl.*, vol. 6, no. 4, pp. 587–601, Dec. 2022, doi: 10.1007/s41315-022-00247-x.
- [19] S. H. Abbasi, K. Waqar, A. Mahmood, and M. Imran, "Flight control design of a flapping wing UAV flying in gusts inspired from covert feathers of birds," *J. Micro Bio Robot.*, vol. 19, nos. 1–2, pp. 47–57, Dec. 2023, doi: 10.1007/s12213-023-00157-6.
- [20] W. Send, M. Fischer, K. Jebens, R. Mugrauer, A. Nagarathinam, and F. Scharstein, "Artificial hinged-wing bird with active torsion and partially linear kinematics," in *Proc. 28th Int. Congr. Aeronaut. Sci.*, 2012, pp. 1–10.
- [21] D. C. Karnopp, D. L. Margolis, and R. C. Rosenberg, System Dynamics: Modeling and Simulation of Mechatronic Systems. Hoboken, NJ, USA: Wiley, 2000.
- [22] V. T. Mai, F. Jani, K. A. Alattas, E. Ghaderpour, and A. Mohammadzadeh, "A robust finite-time fault-tolerant tracking control for quadrotor attitude system with stochastic actuator faults and input delays," *IEEE Access*, vol. 13, pp. 64627–64637, 2025, doi: 10.1109/ACCESS.2025.3559180.
- [23] J. R. S. Benevides, M. A. D. Paiva, P. V. G. Simplício, R. S. Inoue, and M. H. Terra, "Disturbance observer-based robust control of a quadrotor subject to parametric uncertainties and wind disturbance," *IEEE Access*, vol. 10, pp. 7554–7565, 2022, doi: 10.1109/ACCESS.2022.3141939.
- [24] K. Zhou and J. C. Doyle, Essentials of Robust Control. Upper Saddle River, NJ, USA: Prentice hall, 1998, pp. 26–290.
- [25] B. Lee, D. Hyun, J. Kim, S. Lee, and J. Ban, "Design of robust H_∞ guaranteed cost controller of quadrotor UAV for set-point tracking," *IEEE Access*, vol. 12, pp. 126074–126087, 2024, doi: 10.1109/ACCESS.2024.3455757.
- [26] M. Rekik, O. Khaled, K. Grigoriadis, and M. A. Franchek, "LHS-GA based H-Infinity control for robust airfoil flutter suppression," *IEEE Access*, vol. 12, pp. 171500–171512, 2024, doi: 10.1109/ACCESS.2024.3501682.
- [27] J. E. Bluman, C.-K. Kang, and Y. Shtessel, "Control of a flapping-wing micro air vehicle: Sliding-mode approach," J. Guid., Control, Dyn., vol. 41, no. 5, pp. 1223–1226, May 2018.



SADDAM HUSSAIN ABBASI received the B.S. degree from the National University of Sciences and Technology, Pakistan, in 2009, the M.S. degree from UET Taxila, Pakistan, in 2016, and the Ph.D. degree from SS-CASE-IT, Islamabad, Pakistan, in 2022. He has published several scientific papers in high-impact factor journals and conferences. His research interests include bio-inspiration and bio-mimetic designs, modeling and simulation, control system design, bio-

inspired robotics, and gust mitigation systems in UAVs. He is presently working on research of an active gust mitigation system for flapping wing UAVs.





ZAID AHMED SHAMSAN (Senior Member, IEEE) received the B.Sc. degree (Hons.) in electronics and communication engineering from the Sudan University of Sciences and Technology (SUST), in 2002, and the master's and Ph.D. degrees in telecommunication and electrical engineering from Universiti Teknologi Malaysia (UTM), Johor, Malaysia, in 2007 and 2010, respectively. Since 2003, he has been with the Faculty of Engineering and Information Technology,

Taiz University, Taiz, Yemen. From July 2007 to February 2010, he was an Assistant Researcher with the Wireless Communication Center (WCC), Faculty of Electrical Engineering, UTM, focusing on several research projects mainly in the field of frequency spectrum management funded by Malaysian Communications and Multimedia Commission (MCMC), which is successfully completed, in 2010. He was a Postdoctoral Research Fellow with WCC, from April 2010 to April 2012. From 2012 to 2021, he was a member of the International Publishing Unit (IPU), Deanship of Academic Research, IMSIU, and since 2021, he has been the Head of the IPU. He has successfully completed many research projects as a Principal Investigator (PI) and a Co-PI funded by various research agencies in Malaysia and Saudi Arabia. He is currently a Professor with the Department of Electrical Engineering, College of Engineering, Imam Mohammad Ibn Saud Islamic University (IMSIU), Riyadh, Saudi Arabia. He is interested in teaching courses, such as electrical circuits analysis, wireless mobile communication, wireless mobile networks, digital communication, satellite communication, communication electronics, and digital signal processing. He has published several scientific papers in high-impact factor and archival technical journals and conferences. His research interests include LTE-Advanced systems, 5G and 6G systems, UAV technology, orthogonal frequency-division multiplexing technology (OFDM), LMDS system analysis, interference analysis techniques, mathematical modeling for coexistence analysis in wireless networks, frequency spectrum management, wave propagation and antenna, channel prediction, rainfall and dust storm analysis and mitigation, free space optics, and optical communication. He received the Bronze Medal in Geneva Innovation 2021 for his project RFID Lock Security Mechanism.



NOUMAN ABBASI received the B.S. degree from the National University of Sciences and Technology, Pakistan, in 2015. He is currently pursuing the M.S. degree in mechanical engineering. His research interests include autonomous systems and mobile robotics, control system designs, adaptive and robust control strategies, multi-agent robotic systems, soft robotics and flexible mechanisms, MAVs and UAVs, mechatronic systems, and embedded control.

. . .